

Electromagnetic Properties of Multifunctional Composites Based on Glass Fiber Prepreg and Ni/Carbon Fiber Veil

Daniel Consoli Silveira¹, Newton Gomes², Mirabel Cerqueira Rezende^{2,3}, Edson Cocchieri Botelho¹

ABSTRACT: Multifunctional composites combine structural and other physicochemical properties, with major applications in aeronautical, space, telecommunication, automotive, and medical areas. This research evaluates electromagnetic properties of multifunctional composites based on glass fiber woven fabric pre-impregnated with epoxy resin laminated together carbon fiber non-woven veil metalized with Ni. In this way, searching for possible application as radar absorbing structures or electromagnetic interference shielding structures. The scattering parameters, in the frequency range of 8.2 to 12.4 GHz, show that the epoxy resin/glass fiber prepreg allows the transmission of the electromagnetic waves through its microstructure, independently of the glass fiber reinforcement orientation (98% transmission, $S_{24} = -0.09$ dB). However, the carbon fiber/Ni veil shows highly reflector behavior (91% reflection, $S_{22} = -0.43$ dB). Energy dispersive spectroscopy of the veil, before and after nitric acid attacks, confirmed the Ni coating removal from the carbon fiber surface. Still, the scattering parameters show reflector behavior (77% reflection, $S_{22} = -1.13$ dB), attributed to the electrical conductivity of carbon fibers. Multifunctional composites based on glass fiber/epoxy/carbon fiber/Ni veil laminates were processed by hot compression molding. The scattering parameters show that the laminates do not behave as good radar absorbing structures. Nevertheless, the laminates present promising results for application as light weight and low thickness structural composites with electromagnetic interference shielding effectiveness (91.4% reflection for 0.36 mm thickness and 100% for ~ 1.1 mm) for buildings, aircraft, and space components.

KEYWORDS: Composite structures, Microwave absorption, Electromagnetic shielding, Glass fiber reinforced plastics, Carbon fiber reinforced plastics.

INTRODUCTION

Many technological advances in modern society have been achieved since the introduction of advanced and multifunctional materials and structures (Gibson 2012). The development of new multifunctional materials involves the combination of structural requirements with other properties not related to mechanical strength (Gibson 2010; Silveira 2015). Therefore, materials with structural properties may be combined — such as tensile, flexural, shear strength, and fatigue resistance — with non-structural materials possessing active properties, for example, electrical and thermal conductivity, self-healing ability, capability to interact with electromagnetic waves, biodegradability, among others (Chin and Lee 2007; Gibson 2012). The multifunctional composite materials with ability to interact with electromagnetic waves are categorized into 2 major classes: the radar absorbing structures (RAS) and the electromagnetic interference (EMI) shielding materials. Both classes may be developed with the ability to withstand mechanical loads, thereby having structural properties, combined with the inherent property of interacting with the electric and/or magnetic wave fields (Lee *et al.* 2016; Thomassin *et al.* 2013).

RAS act attenuating the electromagnetic wave energy via Joule effect, i.e., electrons, nucleus, permanent and/or induced dipoles of material are forced to move, inducing electric current, friction at molecular level, and, consequently, the Joule effect (Soethe *et al.* 2011). If material employed presents impossibility for free movement at the molecular level, the wave may be also attenuated by its reorientation, entering in contrary phase with the incident electromagnetic field. In this case we have the

1. Universidade Estadual Paulista Júlio de Mesquita Filho – Faculdade de Engenharia de Guaratinguetá – Departamento de Materiais e Tecnologia – Guaratinguetá/SP – Brazil. 2. Departamento de Ciência e Tecnologia Aeroespacial – Instituto Tecnológico de Aeronáutica – Laboratório de Guerra Eletrônica – São José dos Campos/SP – Brazil. 3. Universidade Federal de São Paulo – Instituto de Ciência e Tecnologia – Curso de Engenharia de Materiais – São José dos Campos/SP – Brazil.

Author for correspondence: Daniel Consoli Silveira | Universidade Estadual Paulista Júlio de Mesquita Filho – Faculdade de Engenharia de Guaratinguetá – Departamento de Materiais e Tecnologia | Avenida Dr. Ariberto Pereira da Cunha, 333 – Portal das Colinas | CEP: 12.516-410 – Guaratinguetá/SP – Brazil | Email: danielsilveira.tech@gmail.com

Received: Apr. 04, 2016 | Accepted: Oct. 04, 2016

cancelling of wave (Jacob *et al.* 1995; Zhang *et al.* 2015). The depreciation of wave energy by Joule effect inside the material or by phase cancelling reduces the target detection, since the wave is not reflected or is reflected with less intensity to the microwave source. In this way, this class of material assists military and government institutions by controlling spurious electromagnetic radiation, staying under necessary limits and reaching accordance with their respective laws (Silveira 2016).

Valuable RAS have been developed using multi-layered structures (Lee and Yang 2014; Lee *et al.* 2016) or employing frequency selective surfaces (FSS), wherein periodic geometric patterns are incorporated in conductive material (Wan *et al.* 2015; Lee *et al.* 2016). Generally FSS structures have reduced thickness in comparison with multi-layered RAS (Silveira 2016). Also, there are numerous applications of these materials in electronic industries, telecommunication, computers, wind power generation, medical sector, among others (Jang *et al.* 2014; Qin and Brosseau 2012). Some examples of successful application of absorbing materials are found in aviation field. In this area aircrafts equipped with stealth technology may be mentioned, such as the F-117A one, since this is the first aircraft that holds low detection at low altitude. Going further, the B-2 bomber, the F/A-22, and the F-35 aircraft family may be mentioned (Jenn 2005; Nangia and Palmer 2005).

Multi-layered RAS are based on materials responsible for dielectric losses (Lee *et al.* 2016) and/or magnetic losses (Xu *et al.* 2016). Several investigations on multi-layered dielectric structures have been reported in the literature, e.g., epoxy resin composites loaded with C-based materials, such as granular graphite, fullerenes and carbon fibers (Micheli *et al.* 2010), ferrite composites doped with dielectric lossy material, such as $\text{Ba}_{0.7}\text{La}_{0.3}\text{Co}_2\text{Fe}_{16}\text{O}_{27}$ ferrites (Shen *et al.* 2006), sandwich constructions based on carbon nanotube (CNT) combined with polymethacrylimide (PMI) and carbon/epoxy composite (Choi *et al.* 2012). Multi-layer panels with metallic back plane and dielectric layers are strategically positioned to a quarter of microwave length ($\lambda/4$) from the microwave incidence surface — the last employed for a considerable time and known as Jaumann absorbing structure (Hyde *et al.* 2014). Alternatively, FSS RAS have 3 different and relevant intrinsic features: the effective bandwidth, resonant frequency, and reflection loss (RL), all being dependent on structure characteristics (Lee *et al.* 2016; Zang *et al.* 2015). Also, the investigation on the FSS layer material is essential for the determination of the behavior of the FSS RAS (Silveira 2016; Xu *et al.* 2016), prioritizing

materials with low reflection and transmission of microwave and maximized wave energy absorption.

Another important class of multifunctional materials, with ability to interact with microwaves, includes those that promote protection against EMI, which is a critical problem nowadays due to the development and spread of electronic information and its employment in several electronic devices (Lan *et al.* 2014). EMI structures have their shielding effectiveness (SE) mostly based on the reflection of the electromagnetic wave, with considerable metallic behavior (Seo *et al.* 2004), microwave energy absorption can also be observed on a smaller scale (Mishra *et al.* 2016). The total shielding effectiveness ($\text{SE}_T = \text{SE}_R + \text{SE}_A$) of a material is composed by SE due to reflection (SE_R) and SE due to absorption (SE_A). They can be calculated using scattering parameters results from electromagnetic characterization in a vector network analyzer equipped with wave guide and low-loss cables and connectors (Mishra *et al.* 2016), such as those applied in this research. Going further, the total shielding effectiveness ($\text{SE}_T = 10 \log P_i/P_t$) can be obtained by the logarithmic ratio between incoming power (P_i) from emitting port connected at a wave guide and transmitted power through material (P_t). The result is a negative quantity ($P_t < P_i$) expressed in decibels (dB) as the standard unit (Cao *et al.* 2010; Mishra *et al.* 2016).

In most cases, polymeric matrix materials are transparent to microwaves, thus requiring the addition of conductive fillers into the polymer to improve conductivity and reflectivity (Chen *et al.* 2013; Deng *et al.* 2014). An important consideration lays in the comparison of electrical conductivity among conductive particles dispersed into polymeric matrices and fibers and their respective fabrics combined as layer into polymeric matrices. The proximity between metallic particles dispersed in a polymeric matrix is critical for the formation of conductive pathways (Chan *et al.* 2011; Tang *et al.* 2013). Fiber surfaces, mainly carbon fiber (CF), which presents intrinsic conductivity (Gallo and Thostenson 2015; Tzeng and Chang 2001), ideally ensure the formation of conductive pathways, which in turn can help to optimize the microwave reflection and EMI SE.

Even though good EMI shielding is obtained by adding more CFs in the matrix, higher fiber volume fractions lead to difficulties in the production process with associated high costs. The aforementioned difficulties can be minimized or completely solved by coating the CF surface with thin layers of metal or conducting polymers (Tzeng and Chang 2001; Mishra *et al.* 2016). Mishra *et al.* (2016) presented the development of composites based on polyaniline (PANI) doped with β -naphthalene sulfonic

acid (β -NSA), produced via chemical oxidative polymerization and with CF as filler. SE was calculated using scattering parameters (Par_S) results acquired from vector network analyzer in the frequency range from 8.2 to 12.4 GHz. A maximum of -31 dB was obtained for EMI SE (Mishra *et al.* 2016).

Ni is one of the main metals applied for metallization processes of CF, with cementation and electroless deposition employed as main metallization processes (Chung 2012; Sunitha *et al.* 2016). The strategic positioning of the metalized fabric layer into the composite material may be tailored to control the EMI phenomenon (Silveira 2016). Balaraju *et al.* (2016) carried out extensive research into electroless plating of Ni-based polyalloys over CF, *e.g.*, Ni-P, Ni-Cu-P, and Ni-W-Cu-P, deposited via alkaline citrate bath. The EMI SE results for the quaternary coating presented important values, mainly based on absorption (SE_A) and equal to -37 dB. The effect of electroless plating of Ni-P-Cu alloys onto CF and combined with polyether ether ketone composites (CF/PEEK) was also studied by Su *et al.* (2014). The resulted material presented EMI SE over -76 dB, providing CF/PEEK composite, with Ni-P-Cu coating over fibers, potential for different applications satisfying several requirements of EMI (Su *et al.* 2014).

The objective of this study was to process and characterize multifunctional composites, based on epoxy resin/glass fiber (GF) woven fabric prepreg and CF/Ni veil, a non-woven material, evaluating their behavior as RAS or EMI shielding structure in the microwave band (8.2 to 12.4 GHz). In order to evaluate the application of the processed composites as RAS, the CF/Ni veil was treated with HNO_3 acid for the Ni removal from the CF surface.

MATERIALS AND METHODS

The laminates prepared in this study used glass fiber/epoxy resin prepreg and a CF veil metalized with Ni (CF/Ni veil). The prepreg, code HexPly® F155, was based on GF fabric, plain weave style, impregnated with epoxy resin (cured at $120^\circ C$), from Hexcel Co. The conductive layer was based on CF veil bonded with a polyester resin and metalized with Ni. This material is produced by Advanced Fiber Nonwovens, a group of Hollingsworth & Vose Company, code 8000826. This veil is characterized by weight of 25.4 g/m^2 , thickness of 0.18 mm , and surface electrical resistance equal to $0.25\text{ DC } \Omega/\text{square}$. This unity relates the specific electrical resistance in 2 dimensions for materials with uniform and reduced thickness (Bugnet *et al.* 2001; Joffe and Lock 2010).

Aiming to act upon the microwave reflection and absorption properties of the CF/Ni veil, acid treatments were performed

on the veil surface. This procedure intended to remove or to reduce, in a controlled manner, the Ni content on the CF surface. For this purpose, samples of CF/Ni veil ($7.0\text{ cm} \times 7.0\text{ cm}$) were immersed, separately, in aqueous solution of HNO_3 5.0 mol/L for 2 different times, 45 and 120 min, with moderate manual agitation every 5 min. This procedure resulted in 2 new samples of veil, one attacked in acid solution for 45 min (named V_1) and other treated during 120 min (named V_2). After the acid attacks, the veil samples were washed, being shaken carefully in deionized water and dried in an oven at $60^\circ C$ for 270 min.

Laminates based on GF/F155-epoxy resin prepreg have been used routinely in aeronautical industry, with applications in primary and secondary structures, due to their high modulus (Paiva *et al.* 2005). Table 1 shows the families of laminates processed by hot-compression molding in the present study. The processing was performed at a heating rate of $7.6^\circ C/\text{min}$ up to $115^\circ C$, with an isothermal at this temperature for 100 min. The applied pressure was 0.64 MPa . The used sequence of layers is depicted in Table 1, in whose caption it is possible to identify each composite layer. The laminate composite $P/V_0/P_2$ in Family 1, for example, indicates a prepreg layer (P) followed by a unique veil layer as received (V_0) and 2 prepreg layers (P_2). The composite shown in Family 7 (Table 1) is formed by the combination of 2 laminates, $P_3/V_1/P_4$ and $P/V_0/P_2$. So, during the electromagnetic evaluation, the microwave may reach the composite surface formed by 3 cured prepreg layers (P_3), and, presuming that the microwave travels across the complete thickness of the material, it sequentially encounters the V_1 layer and then 5 layers ($P_4 + P$) of the cured prepreg plus 1 layer of V_0 and finally 2 cured prepreg layers (P_2). The contrary can also occur, with the wave reaching the opposite side of this composite, *i.e.*, reaching P_2 , travelling across the laminate in the opposite direction.

Table 1. Multilayer composites electromagnetically characterized.

Families	Laminates
1	$P/V_0/P_2$
2	$P_3/V_0/P_4$
3	$P/V_1/P_2$
4	$P_3/V_1/P_4$
5	$P/V_2/P_2$
6	$P_3/V_2/P_4$
7	$P_3/V_1/P_4 + P/V_0/P_2$
8	$P_2/V_2/P + P/V_1/P_2 + P/V_0/P_2$

P_n : n layers of cured prepreg; V_0 : 1 layer of original veil as received; V_1 : 1 layer of veil treated with acid solution during 45 min; V_2 : 1 layer of veil treated with acid solution during 120 min; "/": Interfacial region between different layers.

The scanning electron microscopy (SEM) analyses were performed in a ZEISS, EVO series LS15 model, with a microprobe INCAX-act from Oxford-Instruments, resolution of 133 eV at 5.9 keV, for the elemental mapping of chemical composition via energy dispersive spectroscopy (EDS). This accessory was used to evaluate the Ni removal from the CF surface of the treated veil. SEM images were obtained by back scattered electron detector (CZBSD) with 20 kV electron accelerating voltage, working distance (WD) of 8.5 mm, without metallization of the samples.

The electromagnetic characterization of the CF/Ni veil, epoxy resin/GF prepreg, and the processed composites (Table 1) were performed using a vector network analyzer (VNA) from Agilent Technologies, model PNA-L N5230C, with 4 ports for signal generation/capture, frequency generator capacity between 300 kHz and 20 GHz, low-loss cables/connectors, and rectangular waveguide, also from Agilent Technologies. The scattering parameters measurements were performed using 2 of the 4 ports available in the VNA, in the frequency range of 8.2 to 12.4 GHz.

Equations 1 and 2 are related with S_{ii} (microwave reflection on material) and S_{ji} (microwave transmission through the material), respectively (Karmel *et al.* 1998; Nicolson and Ross 1970).

$$S_{ii} = \frac{\text{reflected power at port } i}{\text{incident power from port } i} = \frac{V_i^-}{V_i^+} \Big|_{V_j^+ = \text{null}} \quad (1)$$

$$S_{ji} = \frac{\text{transmitted power at port } j}{\text{incident power from port } i} = \frac{V_j^-}{V_i^+} \Big|_{V_j^+ = \text{null}} \quad (2)$$

Equation 1 relates the total energy generated at port i (V_i^+) of VNA, *i.e.*, microwave energy emitted from port i and incident on the material located at the VNA rectangular sample-holder, with the portion of energy reflected back from the material to the same port (V_i^-). Thus the total energy measured in dB refers effectively to the reflected wave on the material surface, with no energy emitted from port j ($V_j^+ = \text{null}$). In contrast, Eq. 2 relates the total energy generated at port i (V_i^+) of VNA with the total energy that crosses the material thickness, finally achieving the port j (V_j^-) located beyond the material. Also, in this case, the generation of microwave energy from port j is turned off ($V_j^+ = \text{null}$). Equation 2 measures the microwave energy that propagates through the entire thickness of the material. The portion of energy not received at port j refers to the attenuated energy, due to the reflected energy on the material surface returning to the emitting port (S_{ii}) and due to the portion of absorbed energy by the material microstructure (E_a) and the dissipated energy (E_d) in the process, the last being considered null.

Equation 3 allows the conversion of S_{ii} and S_{ji} from dB to percentage (%) of signal attenuation or gain (Lee 1991):

$$\text{Signal gain or loss (\%)} = 100 \cdot \left[1 - 10^{\left(\frac{-dB}{10}\right)} \right] \quad (3)$$

Equation 4 supports the understanding of the relationship between transmittance and reflectivity, more specifically the transmission coefficient (T) and the reflection coefficient (Γ). According to this equation, the highest impedance matching between the veil (Z_L) and the medium of wave propagation (Z_0) the nearest to the unit (1.0) is the ratio between the impedances. Substituting this value ($Z_L = Z_0$) in Eq. 4, we have the sum of the squares of Γ and T equal to 1.0, *i.e.*, the reflection decreases as the transmission through the material increases (Bayrakdar 2011; Liao 1990).

$$1 - \Gamma^2 = \frac{Z_0}{Z_L} T^2, \quad (4)$$

where: Z_0 is the impedance of the medium of wave propagation; Z_L is the intrinsic impedance of the material under research.

RESULTS AND DISCUSSION

ELECTROMAGNETIC CHARACTERIZATION

The electromagnetic behavior of epoxy resin/GF prepreg was measured in 2 different GF orientations, in order to verify the possible influence of the arrangement of GF fibers in the interaction with microwaves in the X-band (8.2 to 12.4 GHz). Figure 1 displays the assessed GF orientations.

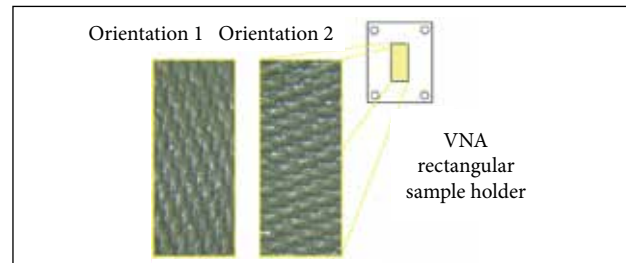


Figure 1. Prepreg GF fabric orientations assessed during electromagnetic characterization.

Figure 2a presents average attenuation equal to -18.93 dB, considering the orientation 1, which, according to Eq. 3 (Lee 1991), corresponds to 98.7% of the attenuation, *i.e.*, only 1.3% of the microwave is reflected.

The same wave-material interaction behavior was identified for the epoxy resin/GF fabric prepreg with orientation 2. As confirmed by S_{22} parameter presented in Fig. 2b, the material is

highly transparent to the microwaves in the X-band, presenting average attenuation of -18.78 dB. This value indicates an attenuation of 98.7%, and only 1.3% of the signal returns to port 2.

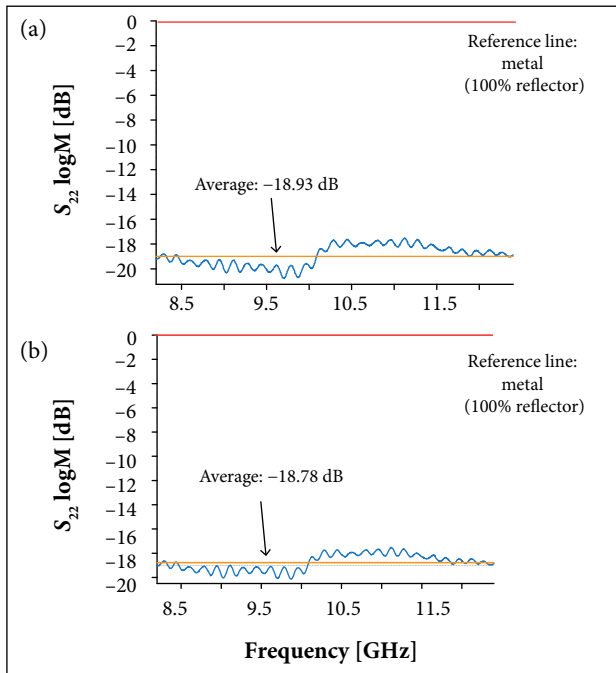


Figure 2. S_{22} curves versus frequency for the epoxy/GF prepreg with GF orientation (a) 1 and (b) 2.

The epoxy resin/GF prepreg transmission (S_{24} and S_{42}) was also measured, and the results confirm the low reflectivity of the material, with average attenuation values through the material of only -0.09 dB, which, according to Eq. 3, indicates that 98% of the microwave is transmitted through the prepreg, independently of the incident wave side on the material (S_{24} is equal S_{42}). The parameter S_{44} was also measured (-18.1 dB for orientations 1 and 2). These results are similar to those shown in Fig. 2. Therefore, the epoxy resin/GF prepreg can be applied during manual lamination process on both sides and at any of the 2 fibers orientations evaluated in this paper, with no impact on the material-microwave interaction. Based on the scattering parameters of the epoxy resin/GF prepreg, it is verified a low reflector behavior (S_{22} equal to S_{44} and highly attenuated) and a high transmission of microwaves through the laminate (S_{24} and S_{42} near to 0 dB of attenuation). Considering the well-known resistance of this material in deteriorative conditions, such as ultraviolet radiation (UV) exposure (Zainuddin *et al.* 2011), moisture absorption (Botelho *et al.* 2008), and thermal degradation (Silveira 2016), the studied prepreg shows potential application as outer layer of EMI structures.

Figure 3 illustrates the electromagnetic properties of the CF/Ni veil, as received, in the frequency range of 8.2 to 12.4 GHz. Taking the average attenuation value of only -0.43 dB for S_{22} as basis, the material in question presents reflector behavior, and 90.7% of wave energy is reflected on the CF/Ni veil surface. This reflector behavior is more pronounced in frequencies below 10.3 GHz as can be seen in Fig. 3a.

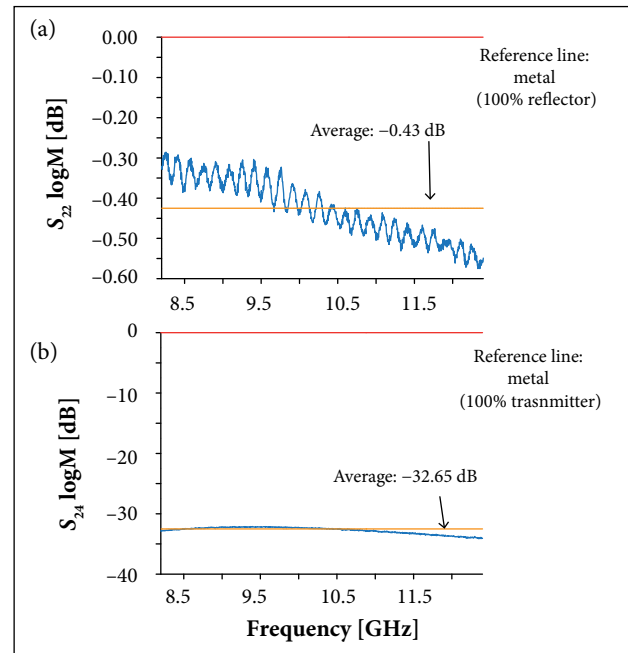


Figure 3. Curves of (a) S_{22} and (b) S_{24} versus frequency of the CF/Ni veil, as received.

Figure 3b presents the S_{24} parameter. The average value of -32.7 dB corresponds to 99.95% of attenuation, i.e., the signal emitted from port 4 does not cross the CF/Ni veil towards port 2. Correlating this result with the S_{22} data, it is clear that the signal is practically all reflected on the veil surface.

The S_{44} and S_{42} parameters were also measured: -0.46 and -32.5 dB average values, respectively. Comparing these values with those presented in Fig. 3, the reflection and transmission present similar behavior independently of the incidence side of the electromagnetic wave on the CF/Ni veil, for frequencies ranging from 8.2 to 12.4 GHz. Based on this information, the veil lamination process can be performed with no worries related with the lamination side previously to the hot-compression molding process.

ENERGY DISPERSIVE SPECTROSCOPY

Once identified the high reflectivity of the CF/Ni veil, as received, acid attacks were conducted, aiming the removal of

the Ni layer from the CF surface. This procedure was an attempt to decrease the reflector behavior of the veil, which, in turn, could lead the material to a condition of greater absorption or transmission of electromagnetic waves in the X-band, providing field of application in RAS. Figure 4 shows representative SEM/EDS chemical mapping in 3 different regions of the CF/Ni veil as received, representative of the veil in its totality. Figure 4a exhibits non-uniform region formed with the presence of deposition and accumulation of Ni (Spectrum 1). Figure 4b presents exposed CF (Spectrum 2), and Fig. 4c is representative of a region with uniform and continuous Ni coating (Spectrum 3).

Table 2 shows the average content, in mass and atomic percentages, of Ni and other chemical elements related to each of the 3 different assessed regions from Fig. 4. The values in Table 2 and the characteristic peaks in Fig. 4a make evident the presence of Ni, indicating high percentage in mass for this metal in the veil, as received. Spectrum from Fig. 4b is related to the black region, with high content (79.2%) of carbon element, where the CF surface is partially exposed. This aspect is attributed to the mechanical removal of Ni layer due to friction between fibers, during the veil handling. This, in turn, is the root cause for the deposition and accumulation of Ni as pointed in Spectrum 1. The chemical content indicated in the spectrum of Fig. 4c, as expected, shows high content of Ni, 72.75% in mass. The EDS spectra also show the presence of O, probably related to the presence of oxides (Burakowski and Rezende 2001) and/or adsorbed gases (An *et al.* 2013).

At sequence, Fig. 5 presents SEM images and results of chemical mapping via EDS in 3 different regions of the CF/Ni veil after the HNO_3 acid attacks.

Table 3 shows the average Ni content determined by SEM/EDS in the veil exposed to the acid attack during 45 min (V_1). Two of the spectra, specifically the Spectra 2 and 3, did not detected the presence of Ni, and the spectrum related to the region pointed in Fig. 5a detected a small percentage of Ni content (0.15% in mass). In addition, it need to be mentioned that the Ni content of the veil attacked in HNO_3 solution during 120 min (V_2) was also surveyed, with no presence of Ni or only traces (average $\sim 0.2\%$ in mass and 0.05% atomic). These results show that the acid attacks in different exposure times were effective in the Ni removal from the CF surface.

The EDS technique of CF/Ni veil after acid attack also detected traces of other elements; among these contaminants, Cl, Si, and Fe were identified. The presence of Fe is attributed to the use of a Fe-C steel support to keep the veil surface suspended during the drying process in the oven, at 60 °C for 270 min. In addition,

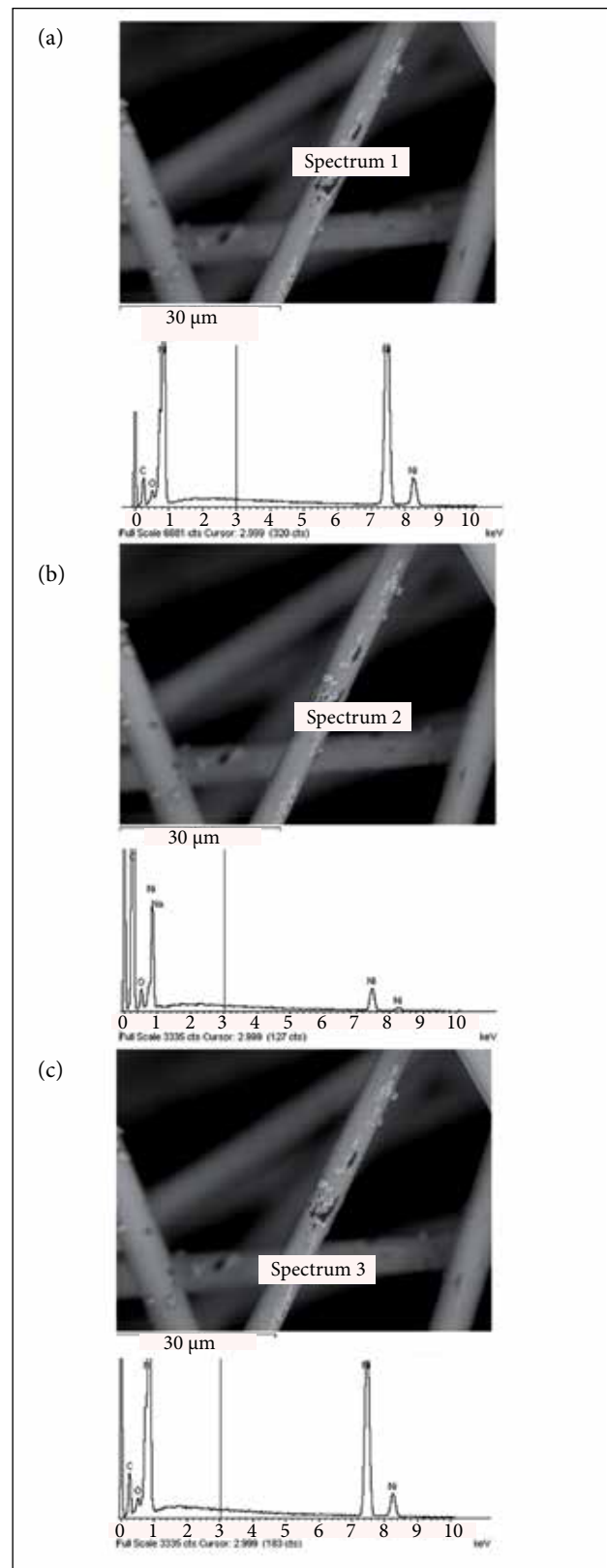


Figure 4. SEM/EDS analyses of the CF/Ni veil as received. (a) Spectrum 1, (b) Spectrum 2, and (c) Spectrum 3.

the comparison of O contents in Tables 2 and 3 shows an increase in this element after the acid attack. This fact can be explained by oxidation processes during acid attack and high temperatures during drying process in the oven, which may add O element on the surface and/or into the samples (An *et al.* 2013). The high carbon content determined is expected. Firstly, because the precursor material of the veil is CF; secondly, due to the presence of polyester polymer, used as binder for the CFs in the veil, as can be observed in SEM images (Spectra 1 and 3 from Fig. 5), which has the C as the main chemical element forming its macromolecules.

The 2 veil samples exposed to acid attacks had their scattering parameters measured. Figure 6a is representative of the S_{22} curves versus frequency for veils V_1 and V_2 . This figure shows that the S_{22} curve for the veils submitted to the acid attack moved downward in relation to the original veil, represented by the black curve in Fig. 6 (-0.43 dB, $\sim 91\%$ of reflectivity), therefore indicating the drop in the reflectivity of the veils exposed to the acid treatments. Specifically for the veil sample exposed to the acid attack during 45 min (V_1), the average S_{22} is -1.13 dB, in other words, an average reflectivity of 77%. Thus, it was found

Table 2. Chemical contents in mass and atomic percentages determined by EDS of the CF/Ni veil as received.

Element	% Mass			% Atomic		
	Figure 4a*	Figure 4b	Figure 4c	Figure 4a	Figure 4b	Figure 4c
C	16.7	79.2	24.5	47.7	88.5	59.16
O	2.2	10.9	2.75	4.8	9.15	4.97
Ni	81.1	9.6	72.75	47.5	2.2	35.87
Na	--	0.3	--	--	0.15	--

*Regions indicated in Fig. 4.

Table 3. Chemical contents in mass and atomic percentages determined by EDS of the CF/Ni veil after the acid attack.

Element	% Mass			% Atomic		
	Figure 5a*	Figure 5b	Figure 5c	Figure 5a	Figure 5b	Figure 5c
C	63.07	84.19	71.8	69.8	88.1	77.8
O	35.87	14.47	26.43	29.8	11.4	21.5
S	0.91	0.52	1.77	0.37	0.21	0.70
Ni	0.15	--	--	0.03	--	--
Si	--	0.19	--	--	0.08	--
Cl	--	0.46	--	--	0.16	--
Fe	--	0.17	--	--	0.05	--

*Regions indicated in Fig. 5.

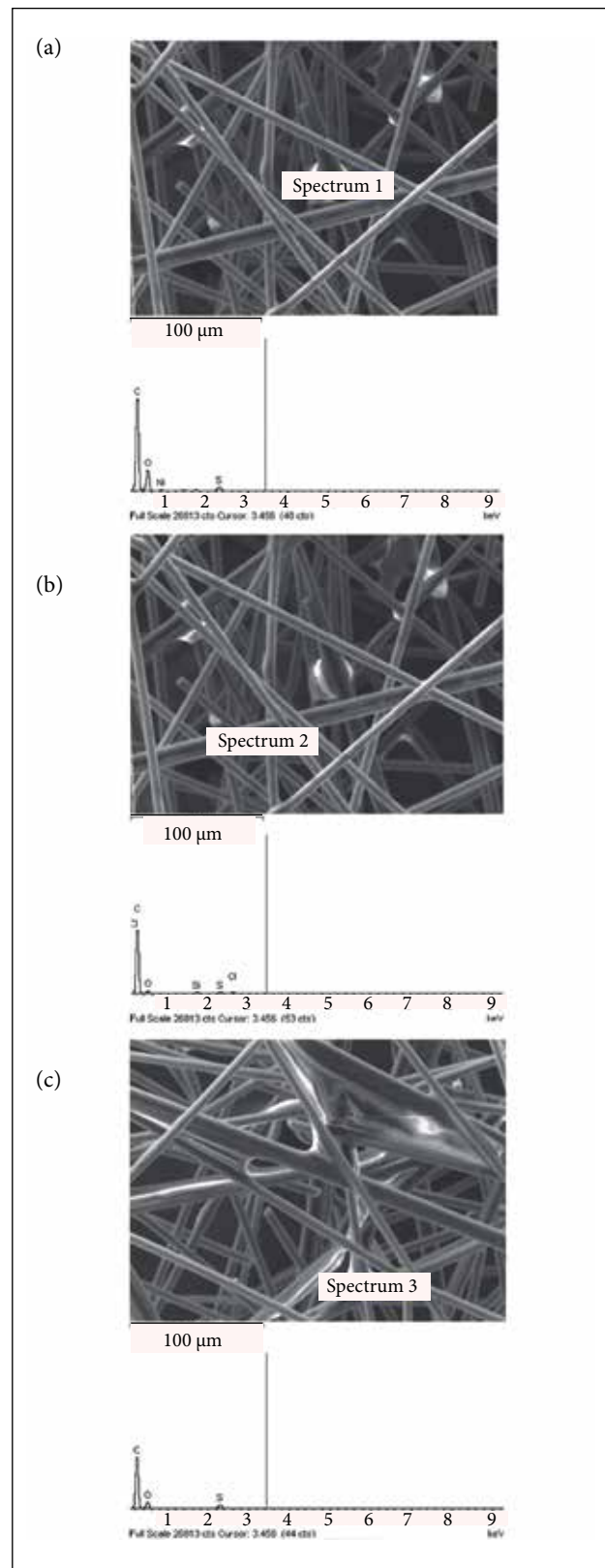


Figure 5. SEM/EDS analyses of the CF/Ni veil after acid attack. (a) Spectrum 1, (b) Spectrum 2, and (c) Spectrum 3.

a maximum reflectivity reduction equal to 14% in comparison with the original CF/Ni veil, as a consequence of the Ni removal. For the veil sample exposed to the acid attack during 120 min (V_2), the average S_{22} is -0.56 dB, corresponding to an average reflectivity of $\sim 88\%$.

The S_{42} transmittance parameters for veils V_0 , V_1 , and V_2 were also measured, and the results are presented in Fig. 6b. The S_{42} values show that the transmittance of the veils increases from V_0 , through V_2 , and upward to V_1 . Therefore veils after acid attacks present lower attenuation of microwaves through its microstructure. This behavior was expected based on S_{22} results and Eq. 4.

Now the study is focused on understanding the electromagnetic behavior of the epoxy resin/GF/CF/Ni laminates when impinged by microwaves. According to the literature, when a wave reaches a structure, wave displacements around its axis of propagation may occur, followed by multiple reflections into the laminate. This phenomenon can contribute to phase cancellation between the incident and the reflected wave, leading to the signal attenuation and approaching the material to the necessary conditions for application in RAS (Zhang *et al.* 2015).

Figures 7 present the S_{22} and S_{44} curves versus frequency for the laminates presented in Table 1. In these figures it is observed that the $P/V_2/P_2$ laminate presents the lowest value of attenuation ($S_{44} \sim 0$ dB), featuring no attenuation and reflectivity close to 100%. The greatest average attenuation occurs for the $P/V_1/P_2$

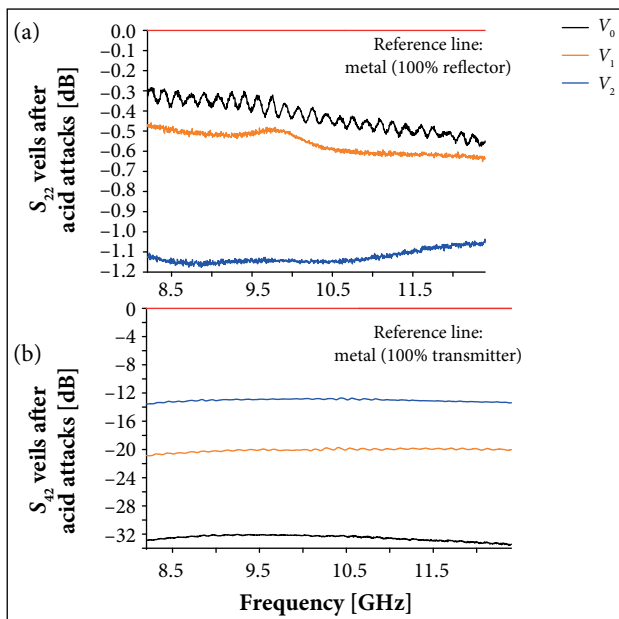


Figure 6. S_{22} (a) and S_{42} (b) curves versus frequency for the CF/Ni veil after acid attacks.

laminate ($S_{22} = -0.39$ dB) when the electromagnetic waves are emitted from port 2, i.e., composite side with 1 prepreg layer and V_1 layer exposed to the incident wave. Thus, the lowest average reflectivity among all these laminates is equal to 91.4%. Also, for the laminate $P_3/V_0/P_4$, it is observed an attenuation peak ($S_{22} = -0.82$ dB) of electromagnetic wave with frequency equal to 9.7 GHz, i.e., 82.8% of reflectivity at this specific frequency.

From the investigation and based on the electromagnetic characterization results, e.g., S_{22} and S_{44} , it was found that the processed laminates do not present desired properties for potential development of RAS. However, the processed laminates combine low thickness (between 0.36 mm for $P/V_1/P_2$ and 1.08 mm for $P_2/V_2/P + P/V_1/P_2 + P/V_0/P_2$), light weight, structural properties, and, as important as the other mentioned properties, significant reflector behavior (low attenuation for S_{ii} parameters, average reflection between 91.4 and 100% of incident microwave in the X-band). In this case, the studied materials present potential for application as multifunctional composites in EMI shielding of buildings, aircraft, and space components.

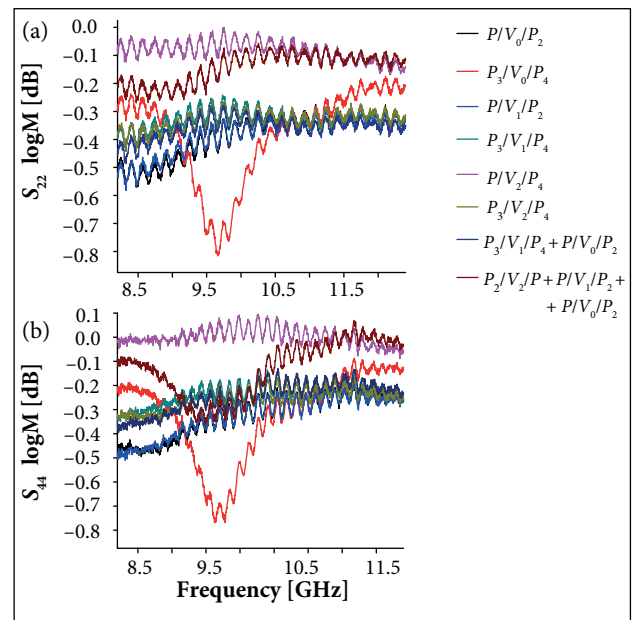


Figure 7. S_{22} (a) and S_{44} (b) parameters versus frequency for GF/epoxy resin/CF/Ni laminates.

CONCLUSIONS

The results presented in this research allow concluding that the epoxy resin/GF fabric prepreg can be applied as outer layer of RAS, since this material allows the transmission, through

its microstructure, of 98.7% of electromagnetic waves in the frequency range of 8.2 to 12.4 GHz. The CF/Ni veil used in this research is predominantly reflective (~91%). Acid treatments of CF/Ni veil were effective in the Ni removal from the CF surface, as confirmed via EDS, with 13.6% of maximum decrease in reflector behavior of the CF veil subjected to acid treatment in 5.0 mol/L HNO₃ solution during 45 min. Hence, even after the complete removal of Ni metallized layer, the CF veil still presented low attenuation for S_{ii} parameters, and it is not adequate for application in RAS, when combined with the epoxy resin/GF fabric prepreg. On the other hand, the results indicate compatibility for processing light-weight and low-thickness reflective multifunctional composites based on epoxy resin/GF/CF/Ni, designed for EMI shielding applications, for example, in buildings, communication, automation, bio-medicine, and aerospace areas. Considering that the studied composites were processed based on continuous GF fabric that presents good mechanical properties, and CF/Ni veil with reflector behavior for microwaves in X-band, multifunctional composites with intrinsic structural and EMI properties have been developed.

REFERENCES

- An H, Feng B, Su S (2013) Effect of monolithic structure on CO₂ adsorption performance of activated carbon fiber-phenolic resin composite: A simulation study. *Fuel* 103:80-86. doi: 10.1016/j.fuel.2011.06.076
- Balaraju JN, Radhakrishnan P, Ezhiselvi V, Kumar AA, Chen Z, Surendran KP (2016) Studies on electroless nickel polyalloy coatings over carbon fibers/CFRP composites. *Surf Coating Tech* 302:389-397. doi: 10.1016/j.surfcoat.2016.06.040
- Bayrakdar H (2011) Complex permittivity, complex permeability and microwave absorption properties of ferrite-paraffin polymer composites. *J Magn Magn Mater* 323(14):1882-1885. doi: 10.1016/j.jmmm.2011.02.030
- Botelho EC, Rezende MC, Pardini LC (2008) Hygrothermal effects evaluation using the iosipescu shear test for glare laminates. *J Braz Soc Mech Sci Eng* 30(3):213-220. doi: 10.1590/S1678-58782008000300006
- Bugnet B, Costa M, Doniat D, inventors; Porous structures having a pre-metallization conductive polymer coating and method of manufacture. 2001 Sept 18. United States Patent US 6290832 B1.
- Burakowski L, Rezende MC (2001) Modificação da rugosidade de fibras de carbono por método químico para aplicação em compósitos poliméricos. *Polímeros* 11(2):51-57. doi: 10.1590/S0104-14282001000200006
- Cao M-S, Song W-L, Hou Z-L, Wen B, Yuan J (2010) The effects of temperature and frequency on the dielectric properties, electromagnetic interference shielding and microwave-absorption of short carbon fiber/silica composites. *Carbon* 48(3):788-796. doi: 10.1016/j.carbon.2009.10.028
- Chan KL, Mariatti M, Lockman Z, Slim LC (2011) Effects of the size and filler loading on the properties of copper- and silver-nanoparticle-filled epoxy composites. *J Appl Polymer Sci* 121(6):3145-3152. doi: 10.1002/app.33798

ACKNOWLEDGEMENTS

The authors are grateful to the Conselho Nacional de Desenvolvimento Científico e Tecnológico (CNPq; Proc.: 303287/2013-6, 303559/2012-8), Coordenação de Aperfeiçoamento de Pessoal de Nível Superior/Programa Professor Visitante Nacional Sênior (CAPES/PVNS), Laboratório de Guerra Eletrônica (LAB-GE) at the Instituto Tecnológico de Aeronáutica (ITA), and Laboratório de Análise de Imagens de Materiais (LAIMat) at the Faculdade de Engenharia of the Universidade Estadual Paulista "Júlio de Mesquita Filho" (UNESP), Guaratinguetá Campus, Brazil.

AUTHOR'S CONTRIBUTION

All authors conceived the idea as well as contributed to design creation, manufacturing, characterizations, data acquisition, results analysis, and comments on the manuscript.

- Chen Z, Xu C, Ma C, Ren W, Cheng H-M (2013) Lightweight and flexible graphene foam composites for high-performance electromagnetic interference shielding. *Adv Mater* 25(9):1296-1300. doi: 10.1002/adma.201204196

- Chin W-S, Lee D-G (2007) Development of the composite RAS (radar absorbing structure) for the X-band frequency range. *Compos Struct* 77(4):457-465. doi: 10.1016/j.compstruct.2005.07.021

- Choi I, Kim J-G, Seo I-S, Lee D-G (2012) Radar absorbing sandwich construction composed of CNT, PMI foam and carbon/epoxy composite. *Compos Struct* 94(9):3002-3008. doi: 10.1016/j.compstruct.2012.04.009

- Chung D-D (2012) Carbon materials for structural self-sensing, electromagnetic shielding and thermal interfacing. *Carbon* 50(9):1972-2012. doi: 10.1016/j.carbon.2012.01.031

- Deng H, Lin L, Ji M, Zhang S, Yang M, Fu Q (2014) Progress on the morphological control of conductive network in conductive polymer composites and the use as electroactive multifunctional materials. *Progr Polymer Sci* 39(4):627-655. doi: 10.1016/j.progpolymsci.2013.07.007

- Gallo G-J, Thostenson E-T (2015) Electrical characterization and modeling of carbon nanotube and carbon fiber self-sensing composites for enhanced sensing of microcracks. *Materials Today Communications* 3:17-26. doi: 10.1016/j.mtcomm.2015.01.009

- Gibson R-F (2010) A review of recent research on mechanics of multifunctional composite materials and structures. *Compos Struct* 92(12):2793-2810. doi: 10.1016/j.compstruct.2010.05.003

- Gibson R-F (2012) Principles of composite material mechanics. 3rd ed. Boca Raton: Taylor & Francis.

- Hyde MW, Bogle AE, Havrilla MJ (2014) Nondestructive characterization of Salisbury screen and Jaumann absorbers using a clamped rectangular waveguide geometry. *Measurement* 53:83-90. doi: 10.1016/j.measurement.2014.03.025
- Jacob J, Chia LHL, Boey FYC (1995) Thermal and non-thermal interaction of microwave radiation with materials. *J Mater Sci* 30(21):5321-5327. doi: 10.1007/BF00351541
- Jang H-K, Choi W-H, Kim C-G, Kim J-B, Lim D-W (2014) Manufacture and characterization of stealth wind turbine blade with periodic pattern surface for reducing radar interference. *Compos Part B-Eng* 56:178-183. doi: 10.1016/j.compositesb.2013.08.043
- Jenn DC (2005) Radar and laser cross section engineering. 2nd ed. Reston: AIAA (Education Series).
- Joffe EB, Lock K-S (2010) Grounds for grounding: a circuit-to-system handbook. IEEE Electromagnetic Compatibility Society. New Jersey: John Wiley & Sons.
- Karmel PR, Colef GD, Camisa RL (1998) Introduction to electromagnetic and microwave engineering. New York: Wiley.
- Lan M, Cai J, Zhang D, Yuan L, Xu Y (2014) Electromagnetic shielding effectiveness and mechanical property of polymer-matrix composites containing metallized conductive porous flake-shaped diatomite. *Compos Part B-Eng* 67:132-137. doi: 10.1016/j.compositesb.2014.06.029
- Lee C-S, Yang C-L (2014) Thickness and permittivity measurement in multi-layered dielectric structures using complementary splitting resonators. *IEEE Sensor J* 14(3):695-700. doi: 10.1109/JSEN.2013.2285918
- Lee S-E, Lee W-J, Oh K-S, Kim C-G (2016) Broadband all fiber-reinforced composite radar absorbing structure integrated by inductive frequency selective carbon fiber fabric and carbon-nanotube-loaded glass fabric. *Carbon* 107:564-572. doi: 10.1016/j.carbon.2016.06.005
- Lee SM (1991) International encyclopedia of composites. New York: VCH Publishers. Vol. 4.
- Liao SY (1990) Microwave devices & circuits. 3rd ed. Upper Saddle River: Prentice-Hall.
- Micheli D, Apollo C, Pastore R, Marchetti M (2010) X-Band microwave characterization of carbon-based nanocomposite material, absorption capability comparison and RAS design simulation. *Compos Sci Tech* 70(2):400-409. doi: 10.1016/j.compscitech.2009.11.015
- Mishra M, Singh AP, Gupta V, Chandra A (2016) Tunable EMI shielding effectiveness using new exotic carbon: Polymer composites. *J Alloy Comp* 688:399-403. doi: 10.1016/j.jallcom.2016.07.190
- Nangia RK, Palmer ME (2005) A comparative study of UCAV type wing planforms-aero performance and stability considerations. Paper presented at: 23rd AIAA Applied Aerodynamics Conference; Toronto, Canada.
- Nicolson AM, Ross GF (1970) Measurement of the intrinsic properties of materials by time-domain techniques. *IEEE T Instrum Meas* 19(4):377-382. doi: 10.1109/TIM.1970.4313932
- Paiva JMF, Mayer S, Rezende MC (2005) Evaluation of mechanical properties of four different carbon/epoxy composites used in aeronautical field. *Mater Res* 8(1):91-97. doi: 10.1590/S1516-14392005000100016
- Qin F, Brosseau C (2012) A review and analysis of microwave absorption in polymer composites filled with carbonaceous particles. *J Appl Phys* 111(061301). doi: 10.1063/1.3688435
- Seo IIS, Chin WS, Lee DG (2004) Characterization of electromagnetic properties of polymeric composite materials with free space method. *Compos Struct* 66(1-4):533-542. doi: 10.1016/j.compstruct.2004.04.076
- Shen G, Xu Z, Li Y (2006) Absorbing properties and structural design of microwave absorbers based on W-type La-doped ferrite and carbon fiber composites. *J Magn Magn Mater* 301(2):325-330. doi: 10.1016/j.jmmm.2005.07.007
- Silveira DC (2016) Obtenção e caracterização de estruturas absorvedoras de micro-ondas baseadas em laminado de fibra laminado de fibra de vidro/resina epoxy/véu de C/Ni (Master's thesis). Guaratinguetá: Universidade Estadual Paulista "Júlio de Mesquita Filho".
- Silveira DC (2015) Processing and characterization of structural and electromagnetic microwave absorber multifunctional composite based on GF/epoxy/CF/Ni. Proceedings of the 2ª Jornada de Iniciação Científica da Pós-Graduação, UNESP, Faculdade de Engenharia de Guaratinguetá [accessed 2016 April 04]. https://www.researchgate.net/publication/282671863_Processing_and_characterization_of_structural_and_electromagnetic_microwave_absorber_multifunctional_composite_based_on_GFEpoxyCFNi
- Soethe VL, Nohara EL, Fontana LC, Rezende MC (2011) Radar absorbing materials based on titanium thin film obtained by sputtering technique. *J Aerosp Technol Manag* 3(3):279-286. doi: 10.5028/jatm.2011.03030511
- Su Y, Zhou B, Liu L, Lian J, Li G (2014) Electromagnetic shielding and corrosion resistance of electroless Ni-P and Ni-P-Cu coatings on polymer/carbon fiber composites. *Polymer Compos* 36(5):923-930. doi: 10.1002/pc.23012
- Sunitha JN, Rajesh CS, Rai SK (2016) Electromagnetic interference shielding effectiveness and electrical conductivity of Ni coated PCABS/PPS composites with reinforcement of carbon fibre. *Polymer Polymer Compos* 24(1):57-63.
- Tang L-C, Wan Y-J, Peng K, Pei Y-B, Wu L-B, Chen L-M, Shu L-J, Jiang J-X, Lai G-Q (2013) Fracture toughness and electrical conductivity of epoxy composites filled with carbon nanotubes and spherical particles. *Compos Part A-Appl S* 45:95-101. doi: 10.1016/j.compositesa.2012.09.012
- Thomassin J-M, Jérôme C, Pardoën T, Bailly C, Huynen I, Detrembleur C (2013) Polymer/carbon based composites as electromagnetic interference (EMI) shielding materials. *Mater Sci Eng R Rep* 74(7):211-232. doi: 10.1016/j.mser.2013.06.001
- Tzeng S-S, Chang F-Y (2001) EMI shielding effectiveness of metal-coated carbon fiber-reinforced ABS composites. *Mater Sci Eng* 30(2):258-267. doi: 10.1016/S0921-5093(00)01824-4
- Wan D, Bie S-W, Zhou J, Xu H, Xu Y, Jiang J (2015) A thin and broadband microwave absorber based on magnetic sheets and resistive FSS. *Progress in Electromagnetics Research C* 56:93-100. doi: 10.2528/PIERC14122203
- Xu H, Bie S, Xu Y, Yuan W, Chen Q, Jiang J (2016) Broad bandwidth of thin composite radar absorbing structures embedded with frequency selective surfaces. *Compos Part A-Appl S* 80:1111-1117. doi: 10.1016/j.compositesa.2015.10.019
- Zainuddin S, Hosur MV, Barua R, Kumar Ashok, Jeelani S (2011) Effects of ultraviolet radiation and condensation on static and dynamic compression behavior of neat and nanoclay infused epoxy/glass composites. *J Compos Mater* 45(18):1901-1918. doi: 10.1177/0021998310394693
- Zang Y, Xia S, Li L, Ren G, Chen Q, Quan H, Wu Q (2015) Microwave absorption enhancement of rectangular activated carbon fibers screen composites. *Compos Part B-Eng* 77:371-378. doi: 10.1016/j.compositesb.2015.03.059
- Zhang J, Xiao P, Zhou W, Hong W, Luo H (2015) Preparation and microwave absorbing properties of carbon fibers/epoxy composites with grid structure. *J Mater Sci Mater Electron* 26(2):651-658. doi: 10.1007/s10854-014-2445-6